Construction of dual-carbon-confined metal sulfide nanocrystals via bio-mimetic reactors enabling superior Fenton-like catalysis

Tao Xu, [a] Yanping Long, [a] Chao He, [a] Xin Song, [b] Weifeng Zhao, [a] [*] and Changsheng Zhao [a,c]

[a] College of Polymer Science and Engineering, State Key Laboratory of Polymer Materials Engineering, Sichuan University, Chengdu, 610065, People's Republic of China

[b] Department of Materials, Department of Bioengineering and Institute of Biomedical Engineering, Imperial College London, London, SW7 2AZ, United Kingdom

[c] College of Chemical Engineering, Sichuan University, Chengdu, 610065, China

[*] *Corresponding author. E-mail: weifeng@scu.edu.cn; zhaoscukth@163.com (Weifeng Zhao)*

Tel.: +86-28-85400453; Fax: +86-28-85405402.

Experimental

Chemicals

κ-Carrageenan, peroxymonosulfate (PMS), tert-butyl alcohol (TBA), p-benzoquinone (pBQ), L-histidine (L-his), β-carotene, 5, 5-dimethyl-1-pyrroline-*N*-oxide (DMPO), 2, 2, 6, 6-tetramethyl-4-piperidinol (TEMP), metal chloride salts (cobalt chloride hexahydrate ($CoCl_2 \cdot 6H_2O$), iron (II) chloride tetrahydrate ($FeCl_2 \cdot 4H_2O$), nickel chloride hexahydrate ($NiCl_2 \cdot 6H_2O$), manganese chloride ($MnCl_2$) and chromium chloride hexahydrate ($CrCl_3 \cdot 6H_2O$)), organic dyes (Rhodamine B (RhB), methyl orange (MO), methyl violet (MV), orange G (OG), methylene blue (MB)), p-chlorophenol (4-CP), sulfamethoxazole (SMX), ciprofloxacin (CIP), tetracycline hydrochloride (TC), Ibuprofen (IBP) and humic acid (HA) were purchased from Aladdin Reagent Co. Ltd. Methanol (MeOH), hydrochloric acid (HCl, 36-38 %), dimethylsulfoxide (DMSO) were purchased from Chengdu Kelong Chemical Reagent Co. Ltd. All the chemicals were analytical grade and used as received.

Fabrication of TMS/carbon nanocomposites via seaweed-mimetic reactor

Zeta potential measurement was carried out with a Zetasizer Nano-ZS90 (Malvern Instruments Ltd., UK). The κ-carrageenan before and after addition of Co (II) were freeze-dried and ground to powders. Then the powders were dispersed to prepare a 1 mg/mL suspension in DI water and the pH value was adjusted (pH 6). The zeta potential measurements were carried out at 25 °C. In order to investigate the effects of different transition metals (TM) on the catalytic performance of catalysts, additional transition metal salts ($CoCl_2$, $FeCl_2$, $NiCl_2$, $MnCl_2$ and $CrCl_3$) were used and pyrolyzed at 900 °C. In order to investigate the effects of Co (II)/SMR ratio on the catalytic performance of catalysts, samples were prepared by varying the initial weight ratio of Co(II)-to-κ-carrageen in the Co@SMR, and pyrolyzed at 900 °C (denoted as C-Co@SMR-900-R, where R represents the weight ratio of Co(II)-to-κ-carrageen). Detailed synthetic parameters/conditions were all compiled in Table S1 below. Additionally, C-SMR-900 was synthesized by following the same procedure as above but without metal assisted.

Table S1. Samples obtained from different synthetic conditions.

Sample	Pyrolysis Temperature (°C)	n of TM (mM)	m (TM): m (carrageen) [a]
C-Co@SMR-800	800	100	1.125:1
C-Co@SMR-900	900	100	1.125:1
C-Co@SMR-1000	1000	100	1.125:1
C-Fe@SMR-900	900	100	0.831:1
C-Ni@SMR-900	900	100	0.994:1
C-Mn@SMR-900	900	100	0.526:1
C-Cr@SMR-900	900	100	1.114:1
C-Co@SMR-900-R0.1	900	10	0.113:1
C-Co@SMR-900-R0.3	900	33	0.375:1
C-SMR-900	900	0	0

[a] Initial weight ratios of reagents used to synthesize the materials.

Preparation of Co_9S_8 nanoparticles (NPs)

A control sample comprising only Co_9S_8 NPs was also synthesized using the following hydrothermal synthetic procedure.[1] First, cobalt (II) acetate tetrahydrate ($Co(Ac)_2 \cdot 4H_2O$, 5 mmol) and thiourea (($NH_2)_2CS$, 5 mmol) were dissolved in ethylene glycol (30 mL). The resulting solution was then transferred into a Teflon-lined stainless-steel autoclave (40 mL) and kept in an oven at 200 ºC for 8 h. The mixture was let to cool down to room temperature and then centrifuged. The resulting black-colored solid powdered product was rinsed with ethanol and let dry at 60 °C.

Preparation of C-Co@SMR-900E

To thoroughly remove the Co_9S_8 nanocrystals in the C-Co@SMR-900, 50 mg of C-Co@SMR-900 were put in 5 M HCl solution at 80 °C for 4 days, followed by washing with deionized water and then drying at 60 °C for 6 h. The obtained sample was named

as C-Co@SMR-900E.

Preparation of C-Co@SMR-900/PVDF composite microfiltration membrane

The C-Co@SMR-900/PVDF composite microfiltration membrane was prepared by directly filtering 10 mg of C-Co@SMR-900 suspensions on a PVDF substrate (Jinteng, 0.22 μm) to obtain a loading amount of 0.18 mg/cm^2.

Calculation of turnover frequencies (TOF) and apparent rate constant (k)

The turnover frequencies (TOF) per metallic atom basis for pollutant removal was calculated through dividing the reaction rate of pollutant degradation by the catalyst concentration.[2]

The apparent rate constant (k) was evaluated by a pseudo first-order kinetics model (eq S1):

$$-\ln (C_t/C_0) = kt \tag{1}$$

where C_0 is the initial pollutant concentration, C_t is the concentration at a certain time t during the degradation process.

The pollutant removal efficiency was calculated using eq S2:

$$\text{Removal efficiency (\%)} = 100 \times (C_0-C_t)/C_0 \tag{2}$$

where C_0 is the initial pollutant concentration, C_t is the concentration at a certain time t during the degradation process.

Electro-chemical measurement

Tafel diagrams were recorded on an electrochemical workstation (CHI 660E, Chenhua Instrument, China) employing a three-electrode system of platinum electrode as the counter, and saturated calomel electrode as the reference electrode. The electrolyte used in this study was 50 mM Na_2SO_4 aqueous solution. All the Tafel diagrams were obtained by polarizing the work electrodes ±200 mV with respect to their open circuit potentials. All the potentials in the Tafel diagrams were with respect to the standard hydrogen electrode (SHE). Electrochemical impedance spectroscopy

(EIS) measurements were conducted on an AUTOLAB electrochemical workstation in the frequency range of 100 kHz - 10 mHz with an amplitude of 5 mV.
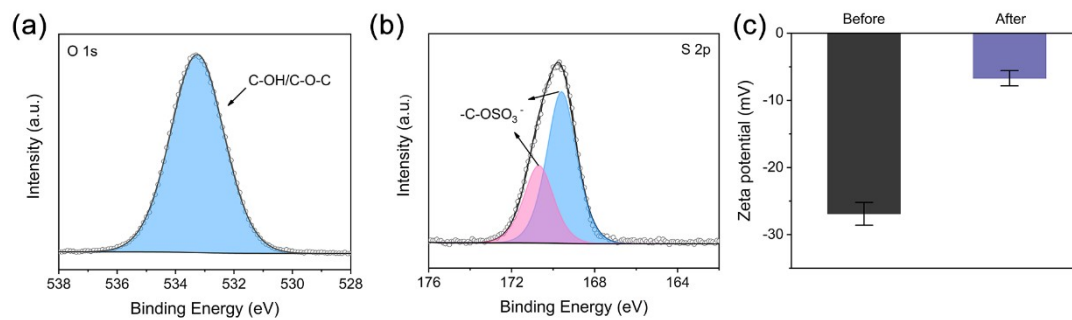
Recyclability and regeneration of C-Co@SMR-900

In each cycle, 1 mg RhB and 10 mg PMS were continuous added to the reaction system. In the recycle test, C-Co@SMR-900 was separated by centrifugation, washed with ethanol (twice) and water (twice), dried in a vacuum oven (60 °C) overnight, and collected for further tests.
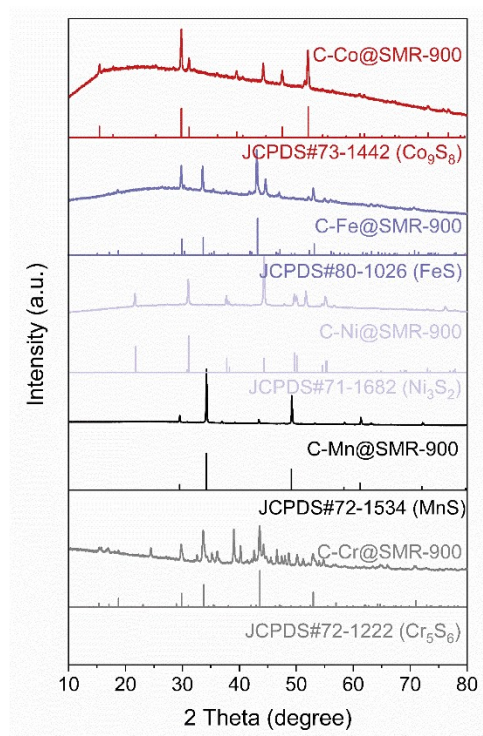
Results
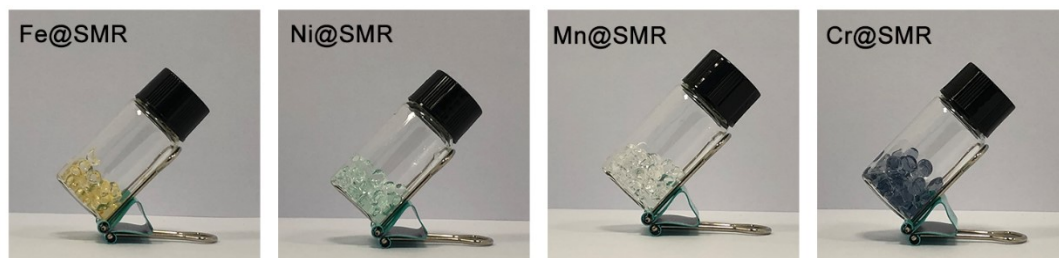
Fig. S1 Photographs of Fe@SMR, Ni@SMR, Mn@SMR and Cr@SMR.

Fig. S2 High resolution O 1s (a) and S 2p (b) XPS spectra of Co@SMR. (c) The zeta potential of the κ-carrageenan in the SMR before and after adding Co (II).

Fig. S3 XRD patterns of the C-Co@SMR-900, C-Fe@SMR-900, C-Ni@SMR-900, C-Mn@SMR-900 and C-Cr@SMR-900.
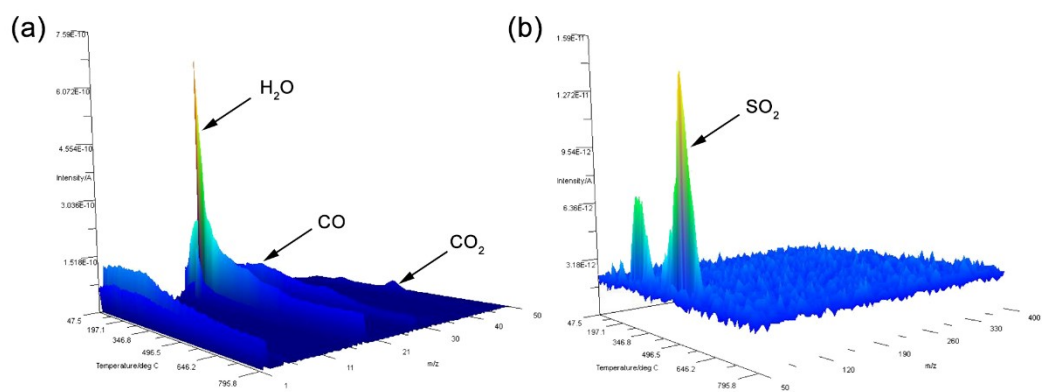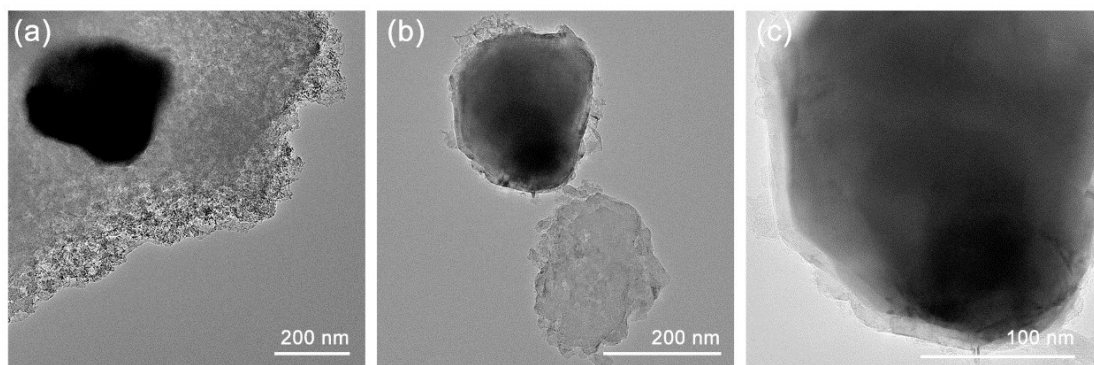
Fig. S4 3D-MS curves of the outlet gases during the *in-situ* sulfidation process.
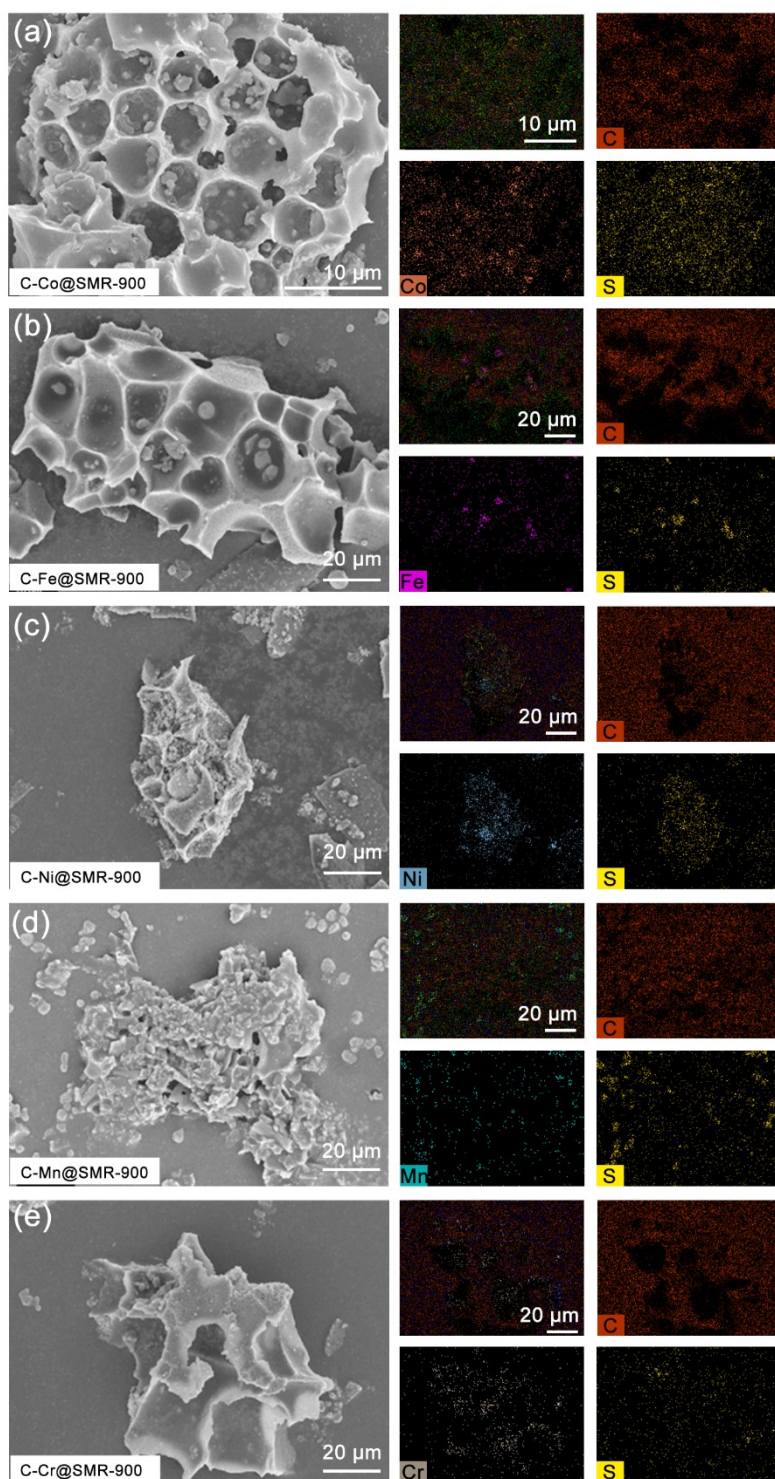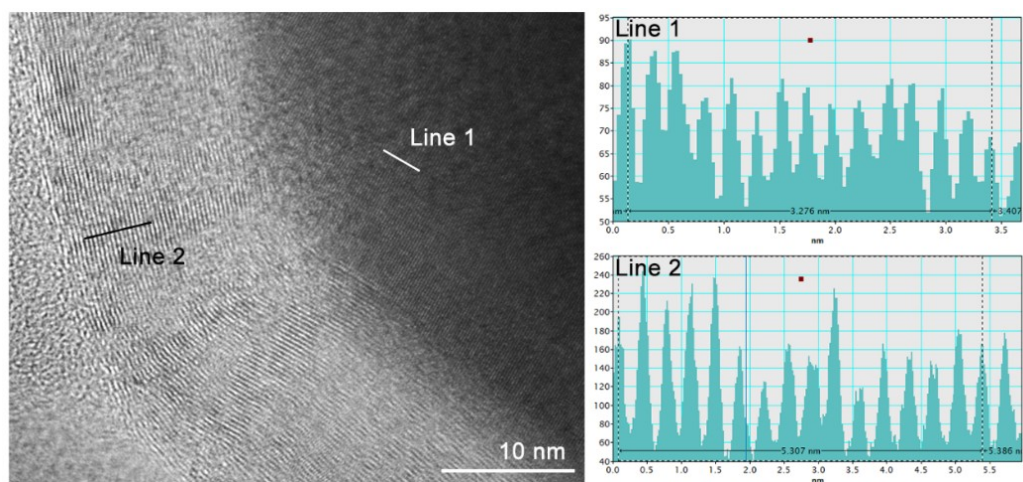
Fig. S5 FESEM image and the corresponding EDS mapping of (a) C-Co@SMR-900, (b) C-Fe@SMR-900, (c) C-Ni@SMR-900, (d) C-Mn@SMR-900 and (e) C-Cr@SMR-900.

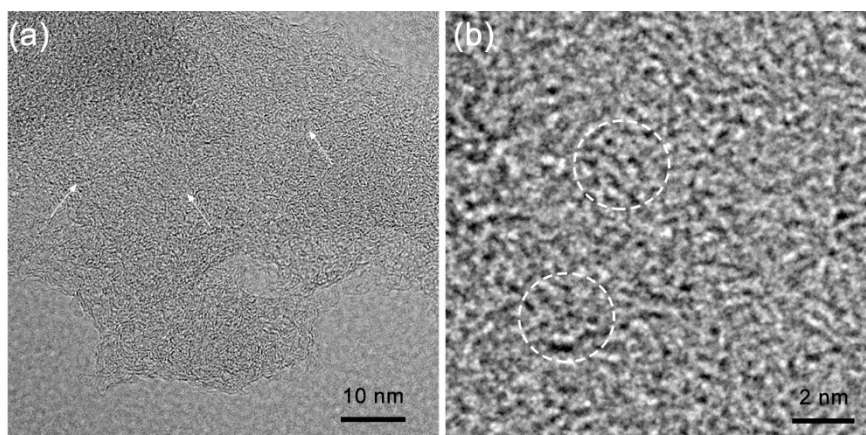**Table S2.** Surface elemental compositions of C-Co@SMR-900 obtained by EDS.

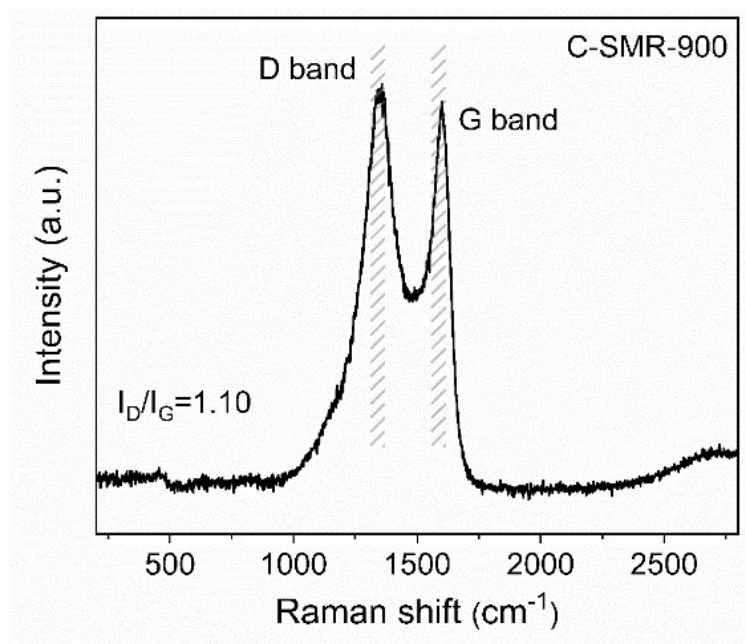|	C (at. %)	O (at. %)	S (at. %)	Co (at. %)
C-Co@SMR-900	82.71	11.65	3.01	2.56

Fig. S6 TEM images of C-Co@SMR-900

Fig. S7 Intensity profiles obtained in the Co_9S_8 nanocrystals (Line 1) and graphitic layer (Line 2).

Fig. S8 HRTEM images of amorphous carbon layers with (a) micropores (b) defects in the C-Co@SMR-900.

**Fig. S9** Raman spectra of the C-SMR-900.

Table S3. Surface areas and pore volume distributions of the as-synthesized catalysts

Sample	BET surface area (m^2 g^{-1})	Total pore volume (cm^3 g^{-1})	Micropore volumes [a] (cm^3 g^{-1})	Meso-macropore volume [b] (cm^3 g^{-1})
C-Co@SMR-800	338.385	0.195	0.108	0.078
C-Co@SMR-900	467.293	0.262	0.121	0.113
C-Co@SMR-1000	576.615	0.414	0.166	0.221

[a] Calculated using t-plot (FHH) method.

[b] Calculated by subtracting the total pore volume with the micropore volumes.
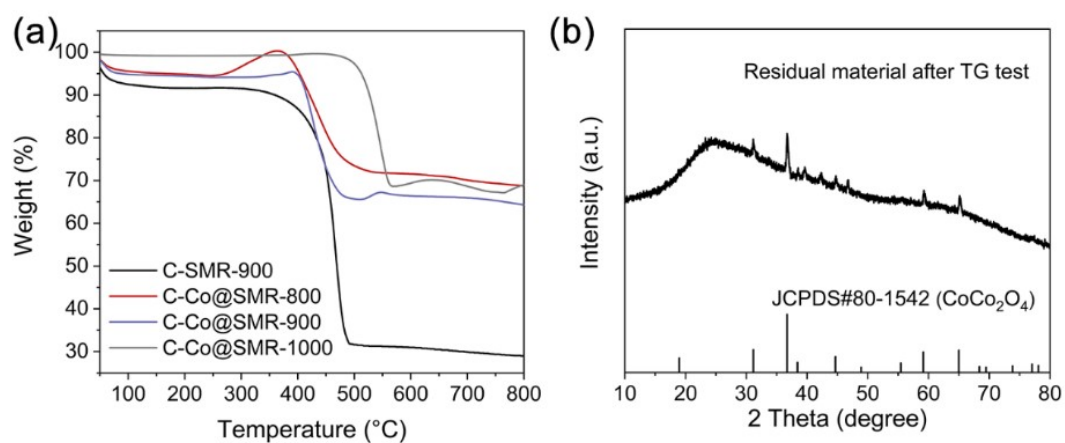
Fig. S10 (a) Thermogravimetric (TG) traces in air in the temperature range of 50 °C to 800 °C for C-SMR-900, C-Co@SMR-800, C-Co@SMR-900 and C-Co@SMR-1000. (b) XRD patterns of the residual material after TG test of C-Co@SMR-900.

**Table S4.** Cobalt loadings of various catalysts obtained by TG and ICP-OES.

| Samples	Cobalt loadings (wt.%)	
	TG	ICP
C-Co@SMR-800	29.18	29.40
C-Co@SMR-900	25.95	26.22
C-Co@SMR-1000	28.03	29.05
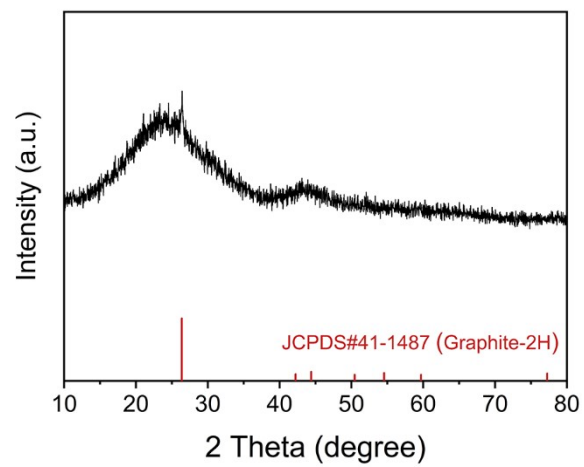
Fig. S11 XRD pattern of C-Co@SMR-900E

**Table S5.** Surface elemental compositions obtained by XPS.

| Samples	C		O		S		Co	
	at. %	wt. %	at. %	wt. %	at. %	wt. %	at. %	wt. %
C-Co@SMR-800	80.40	68.26	15.42	17.44	2.54	10.57	1.65	3.73
C-Co@SMR-900	89.27	79.97	6.89	8.22	1.31	5.75	2.53	6.06
C-Co@SMR-1000	93.06	86.90	4.49	5.58	0.67	3.07	1.78	4.45
C-Co@SMR-900E	88.58	83.20	9.65	12.10	1.64	4.11	0.13	0.61
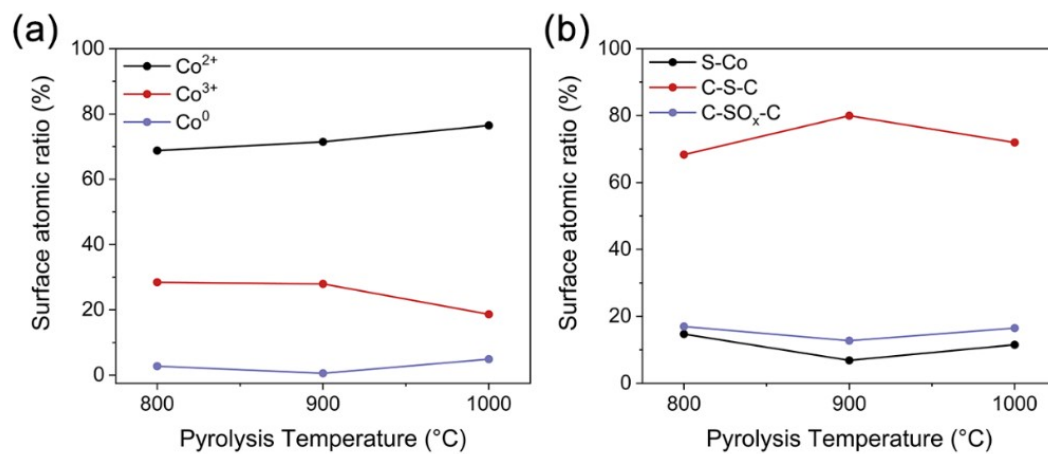
Fig. S12 Percentages of different (a) Co and (b) S species present in C-Co@SMR-900.
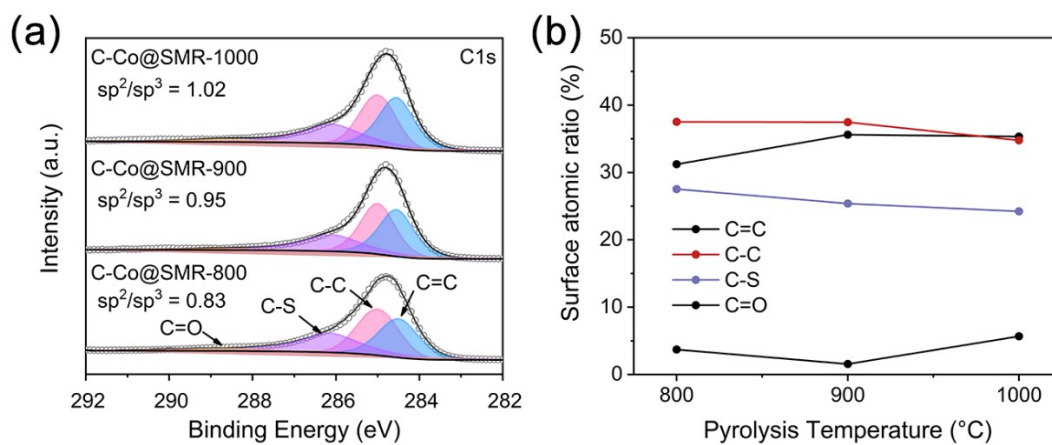
Fig. S13 High-resolution C 1s spectra of C-Co@SMR-800, C-Co@SMR-900 and C-Co@SMR-1000. (b) Changes of different C species in different pyrolysis temperature.
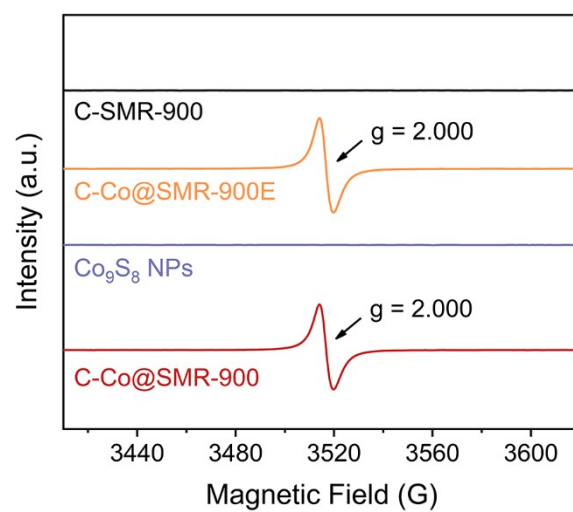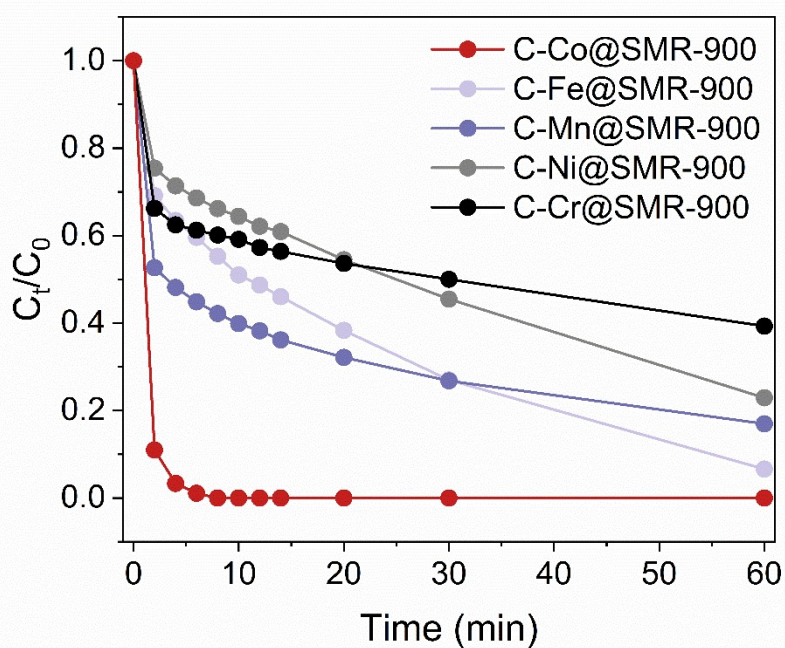
Fig. S14 EPR spectra of C-SMR-900, C-Co@SMR-900E, Co$_9$S$_8$ NPs and C-Co@SMR-900.
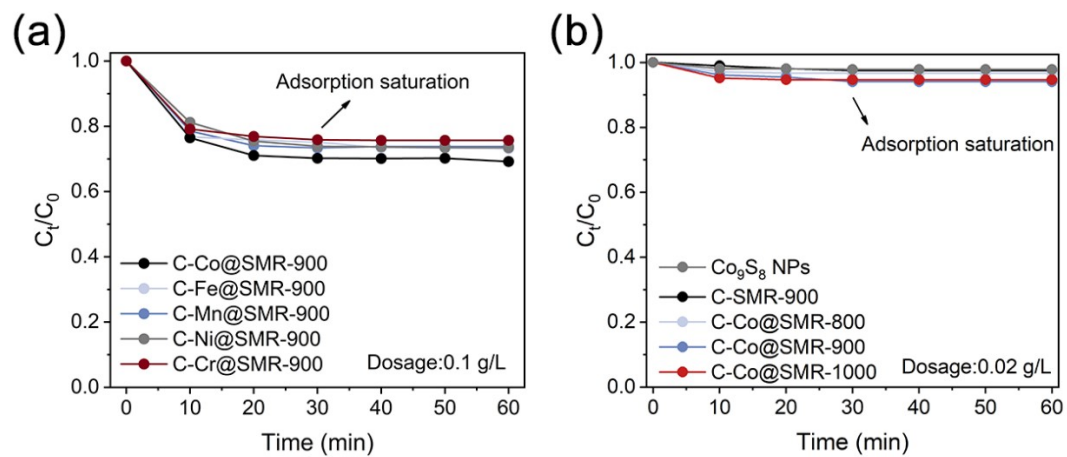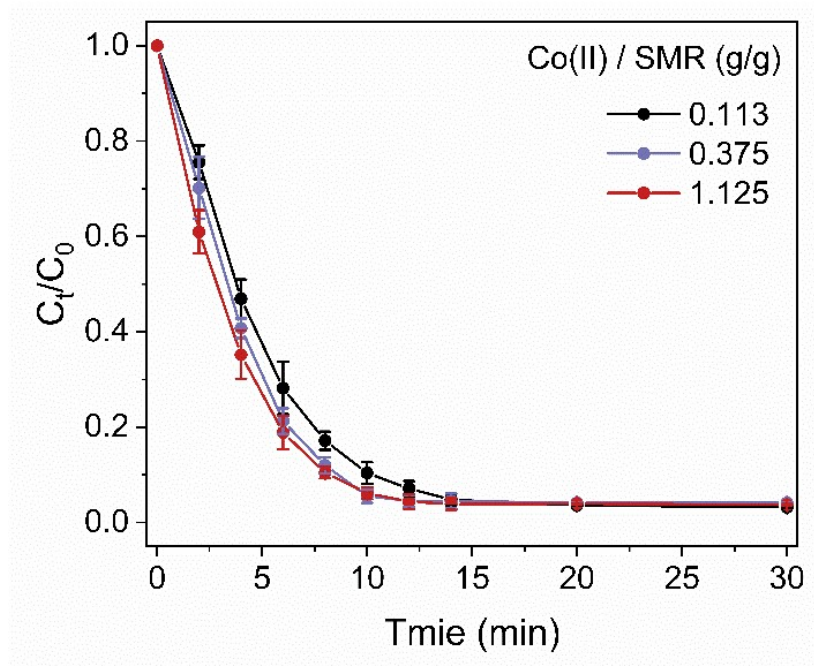
Fig. S15 Time-dependent adsorption curves for RhB by different dosages of catalysts. (a) 0.1 g/L. (b) 0.02 g/L. $[RhB]_0 = 20$ mg/L, initial pH = 6.0, T = 298 K.
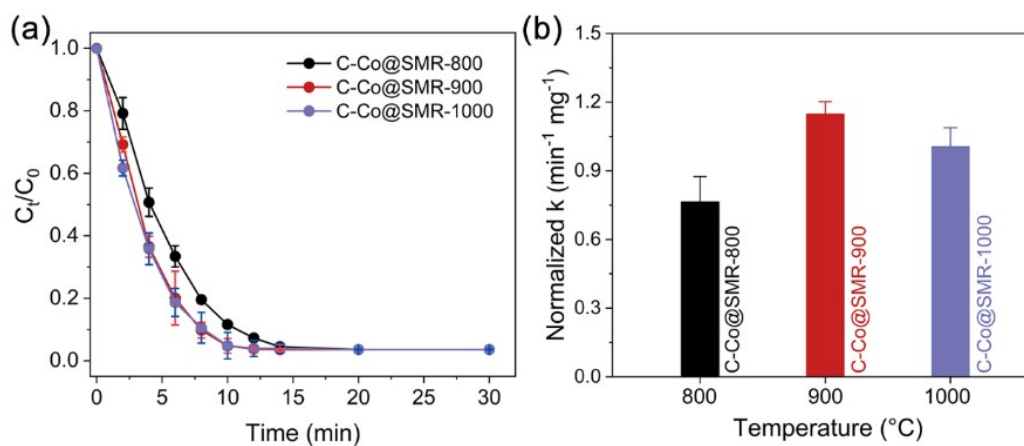
Fig. S16 The degradation curves of RhB catalyzed by C-Co@SMR-900, C-Fe@SMR-900, C-Mn@SMR-900, C-Ni@SMR-900 and C-Cr@SMR-900. Experimental conditions: $[RhB]_0 = 20$ mg/L, $[PMS]_0 = 0.2$ g/L, [C-Co@SMR-900] = [C-Fe@SMR-900] = [C-Mn@SMR-900] = [C-Ni@SMR-900] = [C-Cr@SMR-900] = 0.1 g/L, initial pH = 6.0, T = 298 K.
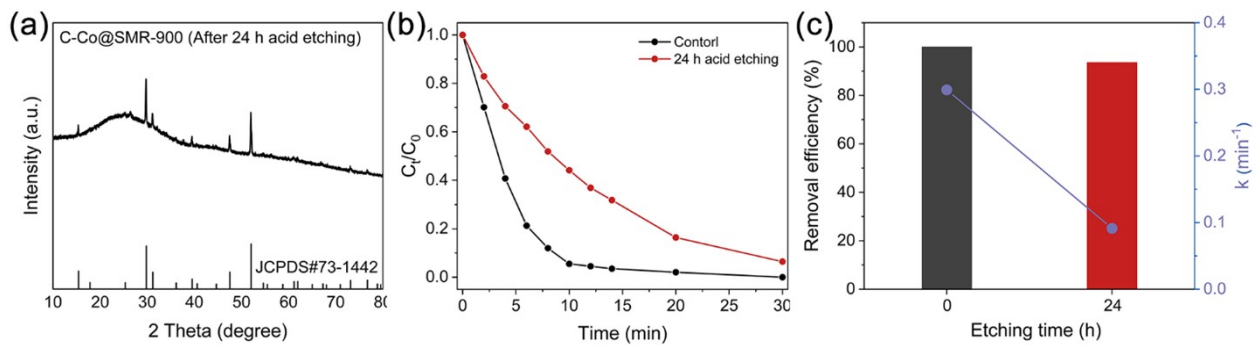
Fig. S17 The degradation curves of RhB catalyzed by C-Co@SMR-900-R0.1, C-Co@SMR-900-R0.3 and C-Co@SMR-900. Experimental conditions: $[RhB]_0 = 20$ mg/L, $[PMS]_0 = 0.2$ g/L, $[Catalyst] = 0.02$ g/L, initial pH = 6.0, T = 298 K.

Fig. S18 (a) The degradation curves of RhB catalyzed by C-Co@SMR-800, C-Co@SMR-900 and C-Co@SMR-1000. (b) Normalized k value by weight of Co. Experimental conditions: $[RhB]_0$ = 20 mg/L, $[PMS]_0$ = 0.2 g/L, [Catalyst] = 0.02 g/L, initial pH = 6.0, T = 298 K.
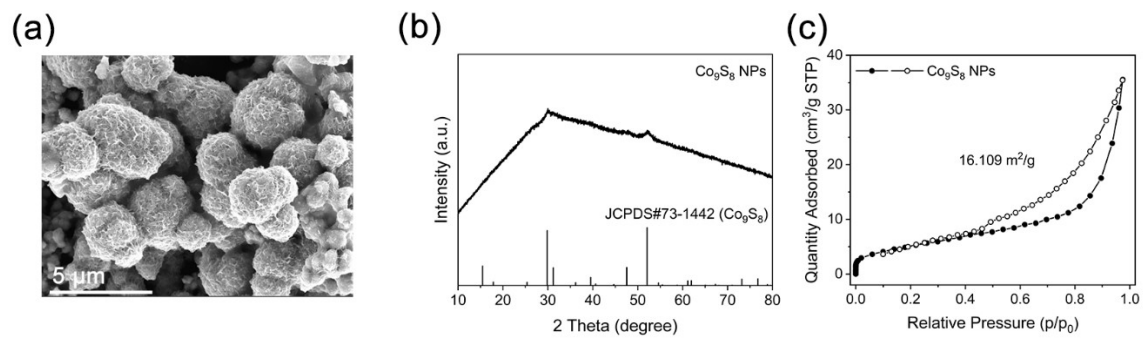
Fig. S19 Different characterization results for Co$_9$S$_8$ NPs synthesized by hydrothermal method. (a) FESEM image. (b) XRD pattern. (c) N$_2$ adsorption/desorption isotherms

Fig. S20 (a) XRD pattern of C-Co@SMR-900 after 24 h acid etching. (b) The degradation curves of RhB catalyzed by acid etched C-Co@SMR-900. (c) The removal efficiency of RhB and the corresponding k value catalyzed by acid etched C-Co@SMR-900 in 30 min.

Table S6. The ICP results for cobalt leaching experiments.

Samples	Cobalt leaching (mg/L)
Co_9S_8 NPs	1.92
C-Co@SMR-800	1.18
C-Co@SMR-900	0.86
C-Co@SMR-1000	0.85
European Union Standard	2.0
Chinese National Standard	1.0
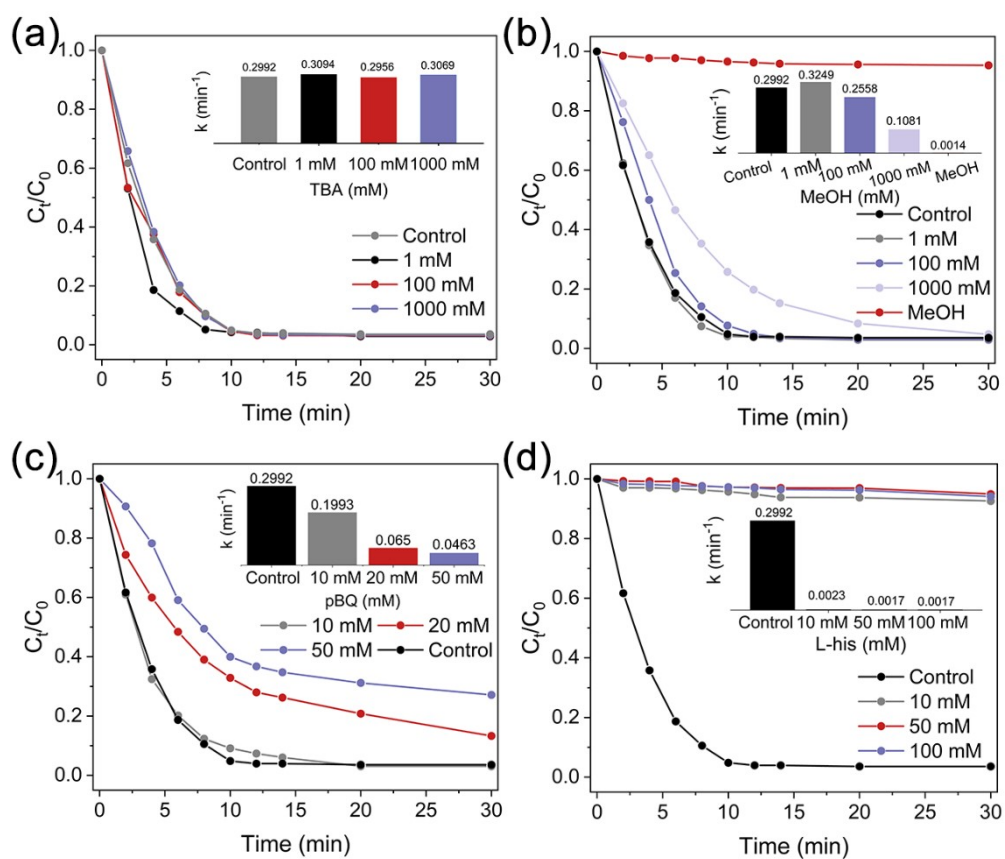
Fig. S21 Effects of different radical scavengers on the RhB degradation. (a) TBA, (b) MeOH, (c) pBQ, (d) L-his. Experimental conditions: $[RhB]_0 = 20$ mg/L, $[PMS]_0 = 0.2$ g/L, [Catalyst] = 0.02 g/L, initial pH = 6.0, T = 298 K.
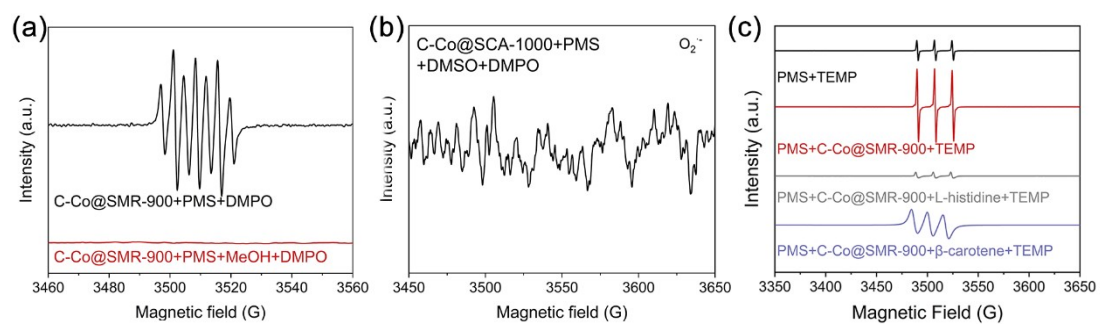
Fig. S22 (a) EPR spectra in C-Co@SMR-900/PMS and C-Co@SMR-900/PMS/MeOH system with DMPO as the trapping agent. (b) Detection of $O_2^{\cdot-}$ in C-Co@SMR-900/PMS/DMSO system with DMPO as the trapping agent.
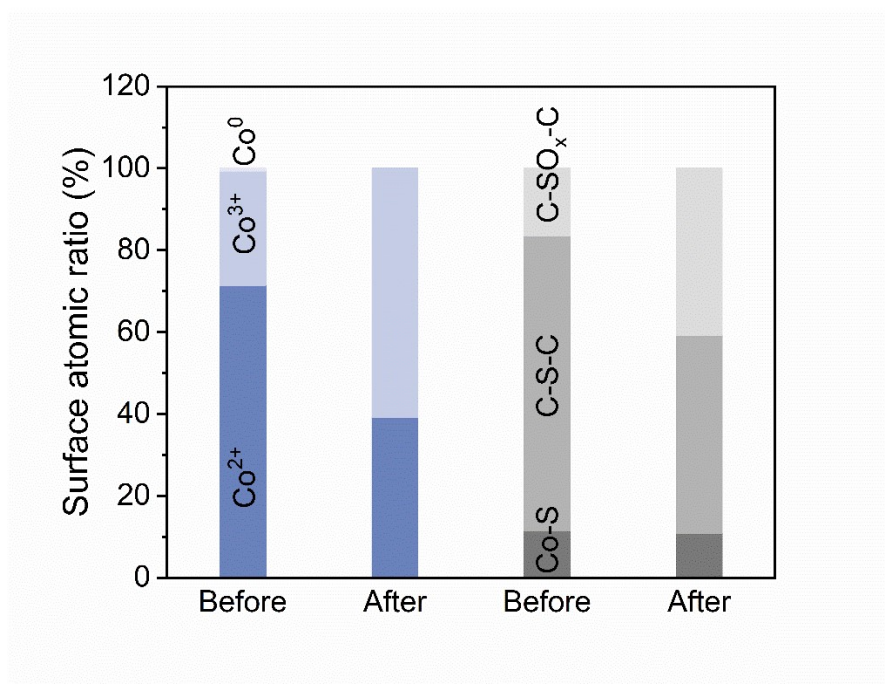
Fig. S23 Corresponding atomic contents of Co and S before and after reaction.
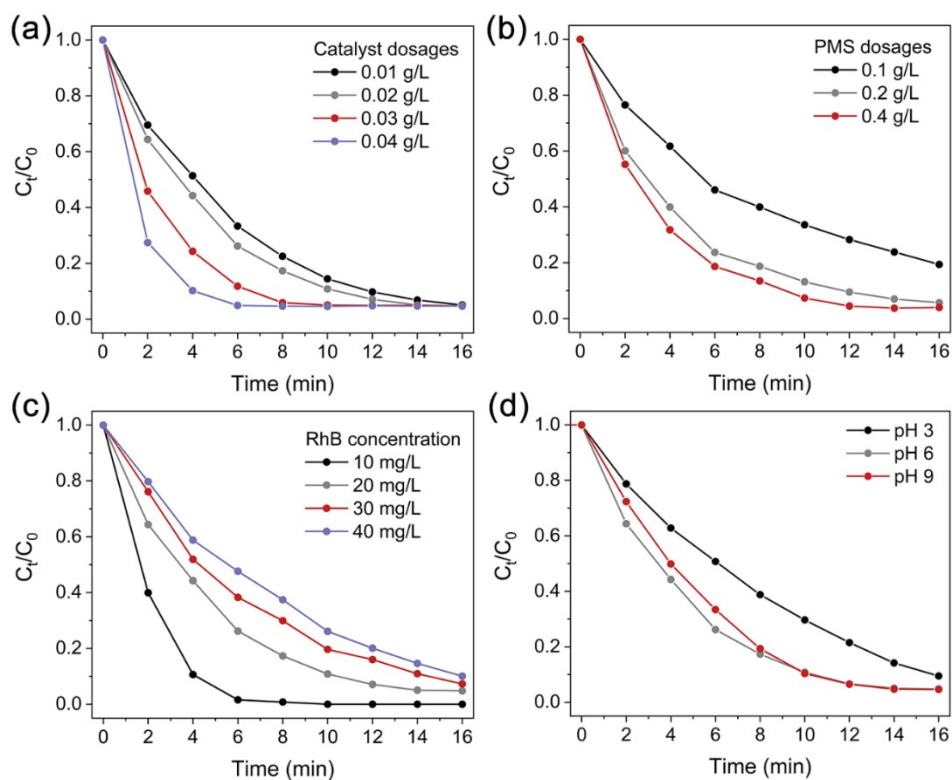
Fig. S24 RhB degradation in C-Co@SMR-900/PMS system considering (a) catalyst dosage; (b) PMS dosage; (c) RhB concentration; (d) pH conditions. Experimental conditions: $[RhB]_0$ = 20 mg/L, $[PMS]_0$ = 0.2 g/L, [Catalyst] = 0.02 g/L, initial pH = 6.0, T = 298 K.
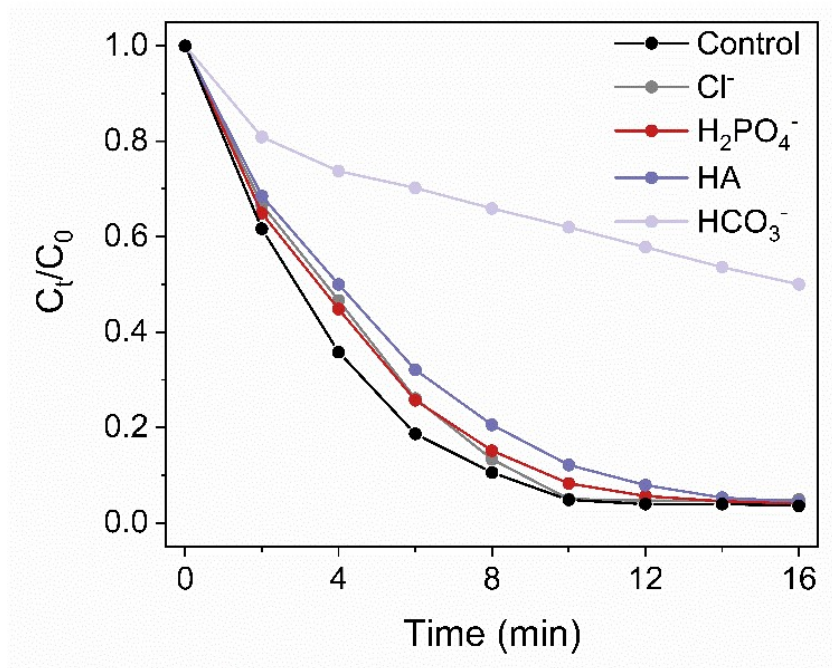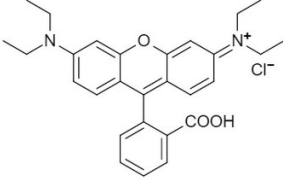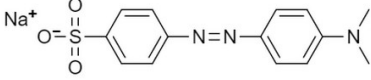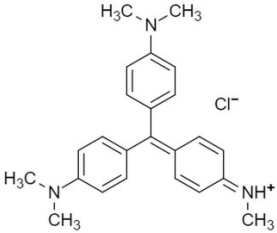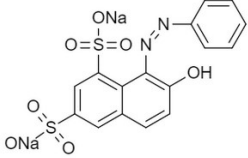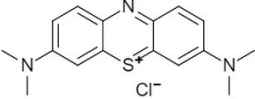
Fig. S25 Effects of inorganic anions and humic acid (HA) on RhB removal. Experimental conditions: $[RhB]_0 = 20$ mg/L, $[PMS]_0 = 0.2$ g/L, $[Catalyst] = 0.02$ g/L, $[Cl^-] = [H_2PO_4^-] = [HCO_3^-] = 5$ mM (if needed), $[HA] = 5$ mg/L (if needed), initial pH = 6.0, T = 298 K.
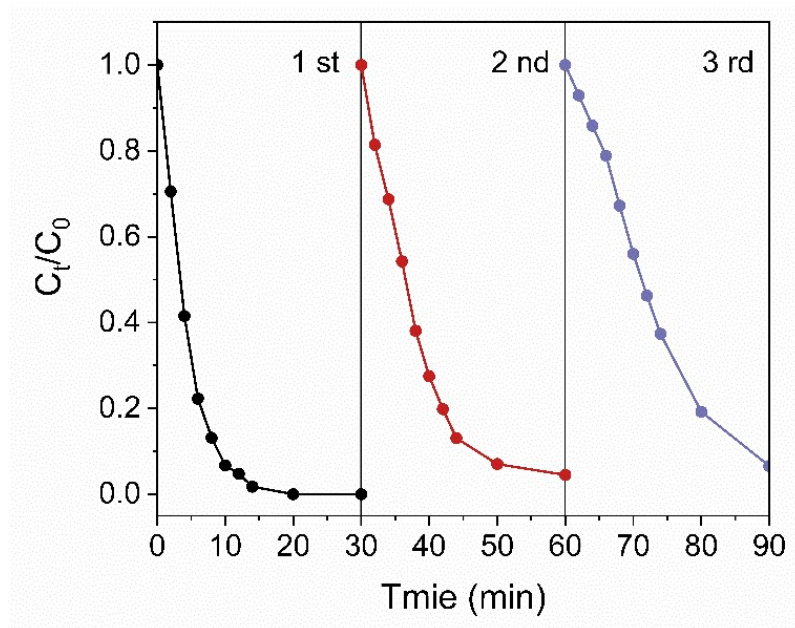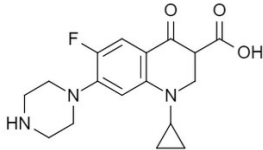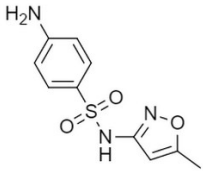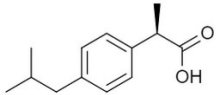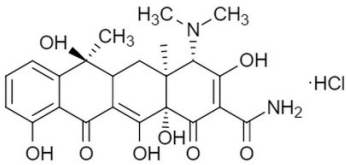
Fig. S26 Recyclability of C-Co@SMR-900 for RhB removal. Experimental conditions: $[RhB]_0 = 20$ mg/L, $[PMS]_0 = 0.2$ g/L, $[Catalyst] = 0.02$ g/L, initial pH = 6.0, T = 298 K

Table S7. UV-vis analysis conditions.

Compounds	Structure	Maximum absorption wavelength (nm)
RhB		554
MO		464
MV		584
OG		478
MB		664

Table S8. HPLC analysis conditions.

Compounds	Structure	Mobile phase	Flow rate (mL/min)	Absorption (nm)	Retention time (min)
4-CP		DI water/Methanol, (30/70, v/v)	1	225	6.27
CIP		DI water/Acetonitrile containing 0.1% formic acid, (78/22, v/v)	1	280	2.74
SMX		Acetonitrile/ Phosphate buffer (0.01M, pH 3), (54/46, v/v)	1	264	4.68
IBP		Acetonitrile/ Phosphate buffer (0.01M, pH 3), (60/40, v/v)	1	220	8.94
TC		Acetonitrile/ Phosphate buffer (0.01M, pH 3), (82/18, v/v)	1	360	2.43
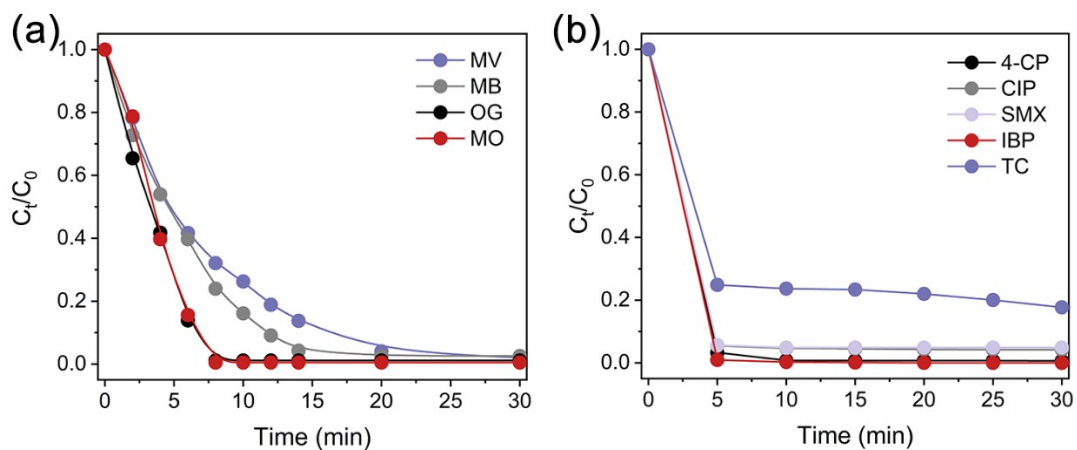
Fig. S27 The degradation curves of (a) dyes and (b) phenol and pharmaceuticals catalyzed by C-Co@SMR-900, [pollutants]$_0$ = 20 mg/L, [PMS]$_0$ = 0.2 g/L, [C-Co@SMR-900] = 0.02 g/L, initial pH = 6.0, T = 298 K.

Table S9. The catalytic performance comparison of recently reported Fenton-like catalysts for RhB degradation. The turnover frequency (TOF) was calculated through dividing the reaction rate of pollutant degradation by the catalyst concentration.

Catalyst dosage (g L^{-1})	PMS^a/H$_2$O$_2^b$ dosage (g L^{-1})	Pollutant (mg L^{-1})	Reaction time (min)	Removal efficiency (%)	Turnover frequencies (min^{-1})	Ref.
C1B2O-5 (0.8)	0.2^a	RhB (25)	180	63.6	0.005	[3]
ASMn-Nb (0.2)	0.5^a	RhB (20)	60	99.7	0.43	[4]
MnO$_2$/Fe$_2$O$_3$ (0.06)	0.25^a	RhB (10)	20	100	3.85	[5]
5% Ca-Fe$_2$O$_3$ (0.5)	0.2^a	RhB (10)	120	99	0.0736	[6]
CA (0.2)	0.3^a	RhB (20)	100	90	0.351	[7]
Fe-Co-Co PBA@PmPDs (0.1)	0.4^a	RhB (15)	60	90.3	0.42	[8]
CoFe$_2$O$_4$/TNTs (0.2)	4^a	RhB (100)	30	100	0.3365	[9]
A-Boron (0.2)	0.15^a	RhB (10)	60	90	0.178	[10]
Cal-ZIF-67/AC(0.12)	0.35^a	RhB (60)	60	98	0.4892	[11]
NH$_3$-S600-KOH (0.2)	0.25^a	RhB (20)	40	100	0.497	[12]
AgBiO$_3$/GO/NCDs-2 (0.5)	0.6^a	RhB (10)	10	95.35	0.1104	[13]
Co(II) doped TiO$_2$ (0.5)	0.3^a	RhB (50)	40	99	0.496	[14]
1% Co-g-C$_3$N$_4$ (0.4)	0.04^a	RhB (10)	25	99	0.3308	[15]
BFO-30 (0.2)	0.4^a	RhB (10)	50	99	0.495	[16]
30%-CNTs-Fe-Mn-0.5 (0.1)	0.4^a	RhB (15)	60	95	0.42	[17]
g-C$_3$N$_4$/MgO (0.2)	1.02^b	RhB (10)	420	91	2.1145	[18]

MnFeO$_2$@OA/PS Janus particles (0.15)	2[b]	RhB (10)	600	95	0.0198	[19]
Co-HAP-2 (0.2)	0.014 [b]	RhB (40)	12	93.3	0.166	[20]
I-FeN$_x$/g-C$_3$N$_4$-5 (0.5)	2.62[b]	RhB(200)	8	100	1.093	[21]
Cu-C$_3$N$_4$ (1)	1[b]	RhB (4.79)	5	100	1.64	[22]
P-PFeCo (2)	0.1	RhB(20)	8	100	0.4	[23]
C-Co@SMR-900 (0.02)	0.2[a]	RhB (10)	14	100	34.525	This work
C-Co@SMR-900 (0.02)	0.1[a]	RhB (20)	14	83	4.94	This work
C-Co@SMR-900 (0.02)	0.2[a]	RhB (20)	14	100	15.05	This work
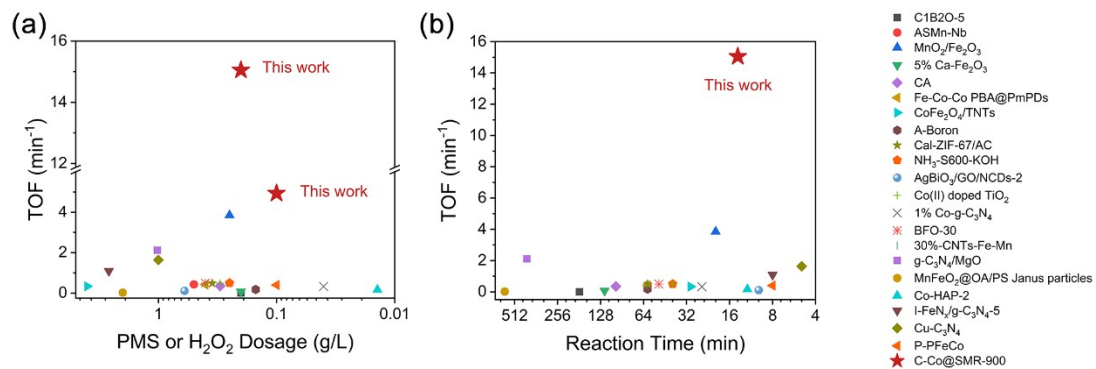
Fig. S28 Summary of catalytic performances of some recently reported catalysts under different reaction conditions (PMS or H$_2$O$_2$ dosage and reaction time)

Table S10. The catalytic performance comparison of recently reported metal sulfide/carbon-based Fenton-like catalysts.

Catalyst dosage (g L^{-1})	PMS^a/$H_2O_2^b$ dosage (g L^{-1})	Pollutant (mg L^{-1})	Reaction time (min)	Removal efficiency (%)	Turnover frequencies (min^{-1})	TOC removal (Reaction time)	Ref.
$Mn_{0.3}Co_{2.7}S_4$ (0.08)	0.3[a]	SMT (55)	120	97	4.54	25%/120 min	[24]
FeS_2 (2)	0.6 [a]	DEP (20)	120	100	0.064	50.5%/120 min	[25]
CoS_2 (0.08)	0.4 [a]	CIP (10)	60	100	1.5	20.7%/60 min	[26]
Co_9S_8@N-S-BC (0.2)	0.5[a]	SMX (20)	240	100	1.73	33.3%/240 min	[27]
Co_9S_8@NSBOC (0.2)	0.2[a]	MB (30)	60	98	0.34	27.59%/60 min	[28]
Co/Co_9S_8@N-S-O-C (0.1)	0.25[a]	SMX (10)	240	100	3.07	30.1%/240 min	[29]
CoS@GN-60 (0.1)	0.1[a]	BPA (20)	8	97.1	6.2	40.64%/8 min	[30]
C-Co@SMR-900 (0.02)	0.2[a]	RhB (20)	14	100	15.05	23.55%/30 min	This work
C-Co@SMR-900 (0.08)	0.2[a]	RhB (20)	14	100	11.06	75.18%/60 min	This work

Table S11. Estimated total cost for preparing 1 g of recently reported Fenton-like catalysts.

Classification	Catalysts	Materials	Amount used (g)	Unit cost (dollar)	Total cost (dollar)	Ref.
Metallic oxides	C-CoCu-HNC [a]	Co(NO$_3$)$_2$·6H$_2$O	2.448	0.098	2.258	[31]
		Cu(NO$_3$)$_2$·3H$_2$O	0.294	0.151		
		2-methyl imidazole	4.189	0.106		
		methanol	306 mL	0.005		
	Co(II) doped TiO$_2$ [a]	CoCl$_2$·6H$_2$O	0.553	0.044	1.389	[14]
		titanium isopropoxide	2.183	0.028		
		glycerol	28.631 mL	0.018		
		ethylenediamine	14.315 mL	0.055		
		Co(NO$_3$)$_2$·6H$_2$O	0.583	0.098		
	CoFe$_2$O$_4$/TNTs [c]	Fe(NO$_3$)$_3$·9H$_2$O	1.614	0.013	0.225	[9]
		citrate acid	0.841	0.008		
		ethanol	N/A	0.005		
		TiO$_2$	0.5	0.013		
		NaOH	6.667	0.020		
	Co-HAP-2 [b]	hydroxyapatite	1	15.387	15.458	[20]
		Co(NO$_3$)$_2$·6H$_2$O	0.728	0.098		
Metal/carbon hybrid	Cal-ZIF-67/AC [b]	Co(NO$_3$)$_2$·6H$_2$O	0.16	0.098	0.155	[11]
		2-methyl imidazole	0.391	0.106		
		methanol	16.5 mL	0.005		
		activated carbon pellets (10–60 mush)	1.2	0.013		
	AgBiO$_3$/GO/NCDs-2 [b]	AgNO$_3$	0.349	2.031	4.413	[13]

		NaBiO$_3$·2H$_2$O	0.734	1.384		
		graphene oxide	0.010	339.657		
		citrate acid	0.005	0.008		
		ethylenediamine	0.002 mL	0.055		
		ethanol	N/A	0.005		
		Fe(NO$_3$)$_3$·9H$_2$O	0.502	0.013		
		50 wt.% Mn(NO$_3$)$_2$	0.890	0.015		
	30%-CNTs-Fe-Mn-0.5 [b]	acetone	157.35 mL	0.004	1.182	[17]
		CNTs	0.2	2.192		
		30 wt.% HNO$_3$	31.47 mL	0.003		
	C-Co@SMR-900 [b]	κ-Carrageenan	0.941	0.020	0.065	This work
		CoCl$_2$·6H$_2$O	1.058	0.044		
		FeSO$_4$·7H$_2$O	0.272	0.009		
Metal cluster	I-FeN$_x$/g-C$_3$N$_4$-5 [c]	2-methyl imidazole	1.284	0.106	0.259	[21]
		polyvinylpyrrolidone	1.175	0.061		
		methanol	3.264 mL	0.005		
		melamine	2.055	0.016		
		ethanol	N/A	0.005		
Single atom	Cu-C$_3$N$_4$	cyanamide	2	0.050	0.143	[22]
		Cu(NO$_3$)$_2$·3H$_2$O	0.287	0.151		
		sewage sludge	N/A	N/A		
Metal-free	NH$_3$-S600-KOH	KOH	2.805	0.012	4.033	[12]
		NH$_4$OH	100 mL	0.040		

[a] calculated by XPS.

[b] calculated by ICP-MES.

[c] calculated by TG.

[d] calculated by EDX spectrum

Table S12. Estimated feasibility and sustainability of recently reported Fenton-like catalysts.

Classification	Catalysts	Harmful solvents	Preparation procedures (steps)	Energy-intensive steps	Ref.
Metallic oxides	C-CoCu-HNC [a]	methanol	7	ultrasonication; high-speed centrifugation	[31]
	Co(II) doped TiO$_2$ [a]	glycerol	4	centrifugation	[14]
	CoFe$_2$O$_4$/TNTs [c]	Ethanol; NaOH solution (10 M)	7	Centrifugation; ultrasonication; evaporation; calcined at 350 °C	[9]
	Co-HAP-2 [b]	-	4	Oven drying; calcined at 500 °C	[20]
	Cal-ZIF-67/AC [b]	methanol	5	Ultrasonication; centrifugation; calcined at 500 °C	[11]
Metal/carbon hybrid	AgBiO$_3$/GO/NCDs-2 [b]	ethanol	9	freeze-drying; centrifugation	[13]
	30%-CNTs-Fe-Mn-0.5 [b]	Acetone; HNO$_3$ solution	6	evaporation; oven drying	[17]
	C-Co@SMR-900	-	4	freeze-drying; calcined at 900 °C	This work
Metal cluster	I-FeN$_x$/g-C$_3$N$_4$-5	Methanol; ethanol	6	Centrifugation; ball milling; oven drying; calcined at 600 °C;	[21]
Single atom	Cu-C$_3$N$_4$	-	2	calcined at 560 °C	[22]

| Metal-free | NH$_3$-S600-KOH | KOH solution (0.5 M); NH$_4$OH solution (7 M) | 4 | Oven drying; calcined at 600 °C | 12 |
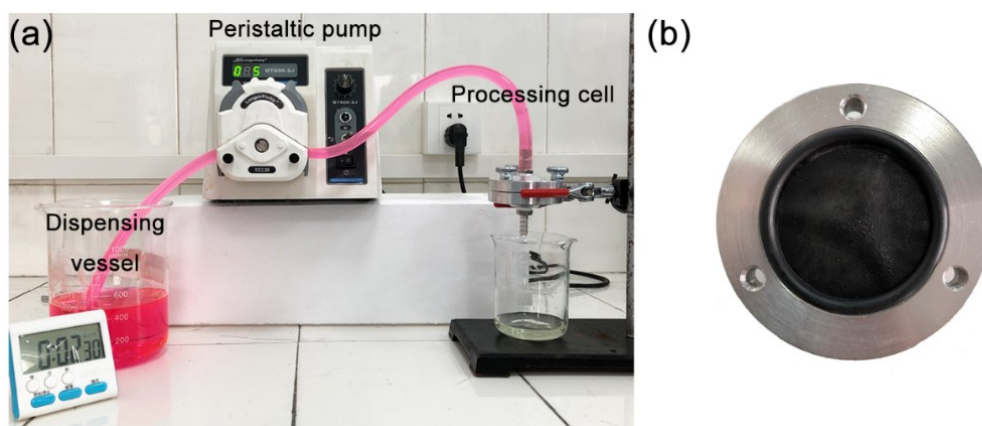
Fig. S29 (a) Photograph of the experimental setup. (b) Photograph of the C-Co@SMR-900/PVDF composite membrane loaded processing cell.

References

1. S. Huang, Y. Meng, S. He, A. Goswami, Q. Wu, J. Li, S. Tong, T. Asefa and M. Wu, *Adv. Funct. Mater.*, 2017, **27**, 1606585.

2. X. Li, X. Huang, S. Xi, S. Miao, J. Ding, W. Cai, S. Liu, X. Yang, H. Yang, J. Gao, J. Wang, Y. Huang, T. Zhang and B. Liu, *J. Am. Chem. Soc.*, 2018, **140**, 12469-12475.

3. Y. Wang, C. Liu, Y. Zhang, W. Meng, B. Yu, S. Pu, D. Yuan, F. Qi, B. Xu and W. Chu, *Appl. Catal., B*, 2018, **235**, 264-273.

4. M. M. Mian, G. Liu, B. Fu and Y. Song, *Appl. Catal., B*, 2019, **255**, 117765.

5. R. Guo, Y. Wang, J. Li, X. Cheng and D. D. Dionysiou, *Appl. Catal., B*, 2020, **278**, 119297.

6. S. Guo, H. Wang, W. Yang, H. Fida, L. You and K. Zhou, *Appl. Catal., B*, 2020, **262**, 118250.

7. L. Jiang, Y. Zhang, M. Zhou, L. Liang and K. Li, *J. Hazard. Mater.*, 2018, **358**, 53-61.

8. L. Zeng, L. Xiao, X. Shi, M. Wei, J. Cao and Y. Long, *J. Colloid Interface Sci.*, 2019, **534**, 586-594.

9. Y. Du, W. Ma, P. Liu, B. Zou and J. Ma, *J. Hazard. Mater.*, 2016, **308**, 58-66.

10. P. Shao, X. Duan, J. Xu, J. Tian, W. Shi, S. Gao, M. Xu, F. Cui and S. Wang, *J. Hazard. Mater.*, 2017, **322**, 532-539.

11. Y. Li, X. Yan, X. Hu, R. Feng and M. Zhou, *Chem. Eng. J.*, 2019, **375**, 122003.

12. M. M. Mian and G. Liu, *Chem. Eng. J.*, 2020, **392**, 123681.

13. X. Yue, X. Miao, X. Shen, Z. Ji, H. Zhou, Y. Sun, K. Xu, G. Zhu, L. Kong, Q. Chen, N. Li and X. He, *J. Colloid Interface Sci.*, 2019, **540**, 167-176.

14. H. Wang, Q. Gao, H. Li, B. Han, K. Xia and C. Zhou, *Chem. Eng. J.*, 2019, **368**, 377-389.

15. L. Wang, X. Guo, Y. Chen, S. Ai and H. Ding, *Appl. Surf. Sci.*, 2019, **467**, 954-962.

16. Z.-S. Zhu, J. Qu, S.-M. Hao, S. Han, K.-L. Jia and Z.-Z. Yu, *ACS Appl. Mater. Interfaces*, 2018, **10**, 30670-30679.

17. X. Tian and L. Xiao, *J. Colloid Interface Sci.*, 2020, **580**, 803-813.

18. L. Ge, Z. Peng, W. Wang, F. Tan, X. Wang, B. Su, X. Qiao and P. K. Wong, *J. Mater. Chem. A*, 2018, **6**, 16421-16429.

19. D. Pan, F. Mou, X. Li, Z. Deng, J. Sun, L. Xu and J. Guan, *J. Mater. Chem. A*, 2016, **4**, 11768-11774.

20. Y. Pang, L. Kong, D. Chen, G. Yuvaraja and S. Mehmood, *J. Hazard. Mater.*, 2020, **384**, 121447.

21. S. An, G. Zhang, T. Wang, W. Zhan, K. Li, C. Song, J. T. Miller, S. Miao, J. Wang and X. Guo, *ACS Nano*, 2018, **12**, 9441-9450.

22. J. Xu, X. Zheng, Z. Feng, Z. Lu, Z. Zhang, W. Huang, Y. Li, D. Vuckovic, Y. Li, S. Dai, G. Chen, K. Wang, H. Wang, J. K. Chen, W. Mitch and Y. Cui, *Nat. Sustainability*, 2021, **4**, 233-241.

23. M. Wang, Q. Gao, M. Zhang, Y. He, Y. Zhang, R. Shen, J. Hu and G. Wu, *J. Mater. Chem. A*, 2021, **9**, 2308-2318.

24. H. Jiang, C. Q. Zhu, Y. Yuan, C. L. Yue, C. Ling, F. Q. Liu and A. M. Li, *Chem. Eng. J.*, 2020, **384**, 123302.

25. Y. Zhou, X. L. Wang, C. Y. Zhu, D. D. Dionysiou, G. C. Zhao, G. D. Fang and D. M. Zhou, *Water Res.*, 2018, **142**, 208-216.

26. W. Q. Li, S. Q. Li, Y. Tang, X. L. Yang, W. X. Zhang, X. D. Zhang, H. X. Chai and Y. M. Huang, *J. Hazard. Mater.*, 2020, **389**, 121856.

27. S. Z. Wang and J. L. Wang, *Chem. Eng. J.*, 2020, **385**, 123933.

28. G. X. Zhu, J. L. Zhu, Q. Liu, X. L. Fu, Z. Y. Chen, K. Li, F. Y. Cao, Q. Qin and M. L. Jiao, *Phys. Chem. Chem. Phys.*, 2021, **23**, 5283-5297.

29. S. Z. Wang, H. Y. Liu and J. L. Wang, *J. Hazard. Mater.*, 2020, **387**, 121669.

30. C. Q. Zhu, F. Q. Liu, C. Ling, H. Jiang, H. D. Wu and A. M. Li, *Appl. Catal., B*, 2019, **242**, 238-248.

31. S. Li, Y. Hou, Q. Chen, X. Zhang, H. Cao and Y. Huang, *ACS Appl. Mater. Interfaces*, 2020, **12**, 2581-2590.